

Comparison of the influence of nitrate ions on the electrochemical behaviour of iron and carbon steels in sulphate solutions

HOUYI MA¹, SHENHAO CHEN^{*1,2}, CHAO YANG³ and JINGLI LUO³

¹*Department of Chemistry, Shandong University, Jinan, 250100, P. R. China,* ²*State Key Laboratory for Corrosion and Protection of Metal, Shenyang, 110015, P. R. China and* ³*Department of Chemical and Materials Engineering, University of Alberta, Edmonton, Alberta, Canada, T6G 2G6*

(Received 21 January 2002)

The effect of nitrate ions on the electrochemical behaviour of iron (ferrite) and two carbon steels (martensite and pearlite) in sulphate solutions of different pH values was investigated by cyclic voltammetry, polarization and electrochemical impedance spectroscopy. The pitting inhibiting effect of nitrate ions on ferrite in sulphate media is pH dependent. Nitrate ions were unable to inhibit the pitting on ferrite in neutral sulphate solutions, but did effectively protect passivated ferrite from pitting in acidic sulphate solutions. No pitting occurred on the surface of the martensite and pearlite specimens in sulphate solutions, regardless of the pH of the solutions. At the open-circuit corrosion potentials, the three materials underwent general corrosion. The impedance spectra for the three materials measured in neutral sulphate solutions containing nitrates and chlorides at the corrosion potentials all showed a capacitive loop, while in acidic sulphate solutions their impedance spectra were greatly reduced in size and displayed at least a low frequency impedance loop (inductive or capacitive loop) besides the well-known high frequency capacitive loop. The variation of the impedance behaviour with pH is explained.

Keywords: pitting, general corrosion, passive film, cyclic voltammogram, polarization curves.

INTRODUCTION

Pitting corrosion is one of the most destructive forms of corrosion among the various types of corrosions. In the mid 1980 s, Smialowska summed up five types of pitting and characterized the features of each type.¹ The most common and most important type of pitting occurs on passivated iron-based alloys in contact with halide-containing aggressive solutions, which involves breakdown of the passive film on iron and its alloys.

It is well known that iron and iron-based alloys are used most widely in industry. Consequently, great attention has been paid to studies on the pitting of iron and its alloys, including carbon steels and stainless steels. Recently, our investigations^{2,3} have shown that, among the ferrite, martensite and pearlite, the passivated ferrite is the most susceptible to

* Corresponding author. Fax: +86-531-8565167, Email: shchen@sdu.edu.cn.

pitting in the $\text{Na}_2\text{SO}_4 + \text{NaCl}$ mixed solutions, followed by passivated pearlite and martensite carbon steels; however, in dilute sulphuric acid, martensite suffers the general corrosion most easily, followed by pearlite and ferrite. These properties are closely related to composition and microstructure of these materials.

It is of important value to study the pitting prevention of metals since pitting does much greater damage to metal products than general corrosion. Newman and Ajjawi's results⁴ have shown that nitrate has a strong inhibition effect on the pitting of stainless steels in neutral chloride solutions. According to Uhlig and Gilman,⁵ nitrate ions can shift the pitting corrosion of Fe–Cr stainless steels to more positive potentials, but some other authors claim that NO_3^- ions scarcely affect the pitting corrosion.^{6,7} Obviously, the pitting inhibition of nitrates has not been interpreted very well. The pitting corrosion inhibition by nitrate ions probably involves competitive adsorption, redox reactions or electroreduction of the nitrate ions,⁴ but none of these could be tested systematically using electrochemical methods. Also, to the best of our knowledge, only a few reports about the effect of nitrate ions on the general corrosion and pitting of iron and carbon steels exist in the literature.

In this study the effect of NO_3^- ions on the general corrosion and pitting of the above-mentioned materials in sulphate solutions of different pH values were investigated using electrochemical methods.

EXPERIMENTAL

The test materials used were 99.98 % pure iron (Aldrich Chem. Co.) and two kinds of carbon steels, martensite and pearlite. The compositions of the two carbon steels are listed in Table I. For the sake of convenience, the three materials are described in this paper as ferrite, martensite and pearlite, respectively.

TABLE I. Chemical compositions of tailings pipe (martensite) and 1080 carbon steel (pearlite) (wt %)

	C	Mn	Si	P	S	Cu	Ni	Mo	V
Martensite	0.47	1.2	0.15	0.05	0.06	0.40	0.40	0.15	0.19
	C				Mn	P_{\max}		S_{\max}	
Pearlite	0.75–0.88				0.60–0.90	0.040		0.050	

The ferrite electrode was made from a pure iron rod of 0.63 cm diameter, and the martensite and pearlite specimens were cut from the corresponding sheets. These specimens were embedded in an epoxy resin mould, and only their test surfaces were allowed to contact the electrolyte. The edges of each sample were coated with an acrylic paint in order to avoid probable crevice corrosion. The area of the test surface of the ferrite, martensite and pearlite electrodes were, respectively, 0.31 cm², 0.41 cm² and 0.45 cm². Prior to each measurement, each test surface was ground with #600 emery paper, subsequently polished with #2000 emery paper, and then rinsed with deionized water and acetone.

All electrolyte solutions were prepared with analytical grade chemicals and triply distilled water.

Electrochemical measurements were performed at room temperature ($\approx 22^\circ\text{C}$) in a three-electrode cell using a Zahner IM6 electrochemical workstation. A platinum black counter electrode of 4 cm² surface area was used as the counter electrode and a saturated calomel electrode (SCE) as the reference electrode to which all the potentials in this paper are referred. The SCE was led to the surface of the working electrode through a Luggin capillary.

The polarization curves were obtained at a potential sweep rate of 0.2 mV s⁻¹ going from the cathodic to the anodic side. The cyclic voltammograms for the three materials in different corrosive solutions were obtained

at a linear potential sweep rate of 5 mV s^{-1} upward from the corrosion potential and then backward to the given potentials. EIS measurements were performed at the corrosion potentials in the frequency range between 60 kHz and 10 mHz with ten points per decade under excitation of a sinusoidal wave of $\pm 5 \text{ mV}$ amplitude.

RESULTS AND DISCUSSIONS

The effect of solution acidity on the pitting of iron and iron-based alloy has been studied by several investigators.^{8–10} However, the influence of the pH of the solution on the inhibition of pitting by nitrate ions was not clear up to now. Systems composed of iron (or iron-based alloys) and sulphate are not self-passivating systems, and the passivation process must be realized by the application of a potential. In addition, the passive state of the metals has to be maintained by applying an anodic potential over the passivating potential. In the presence of chloride ions, the passive films formed on iron or its alloys suffer the attack of pitting, which leads to the breakdown of the passive film and the appearance of pits on the test surfaces. Sulphate ions are unable to effectively inhibit the occurrence of pitting although they may shift, to a certain extent, the pitting potential to more positive values.¹¹ We will first focus on the effect of pH on the inhibition of pitting by nitrate ions in sulphate solutions of different acidity in terms of cyclic voltammetry.

Cyclic voltammetric study

0.1 mol dm⁻³ Na₂SO₄ + 0.1 mol dm⁻³ NaNO₃ + 0.01 mol dm⁻³ NaCl solutions (pH 7.1). The cyclic voltammograms obtained for the ferrite, martensite and pearlite electrodes in Na₂SO₄ + NaNO₃ + NaCl mixed solutions are shown in Fig. 1. It is observed from the cyclic voltammogram of ferrite that the current increased slowly with increasing potential until reaching positively 0.05 V and then it was greatly enhanced by further increasing of the potential during the anodic scan. The anodic voltammogram did not show obvious anodic peaks and passivating behaviour. At potentials higher than 0.05 V, the electrode surface was found to have suffered serious pitting and the rapid increase in current density is probably associated with the occurrence of pitting. This indicates that nitrate cannot protect the ferrite surface from pitting in neutral sulphate solutions. When the potential was scanned negatively, although the current decreased with decreasing potential, the current shown by the reverse scan curve was higher than that shown by the forward scan curve. This phenomenon could be due to the following two causes: (i) the pitting formed on the iron surface during the anodic scan results in a higher surface roughness and (ii) the pits formed were not repassivated during the reverse scan. The latter may be proved by the fact that no common hysteresis appeared in the voltammogram.¹²

The voltammogram of the martensite electrode is similar to that of the pearlite electrode, and both of them are distinctly different in shape to the voltammogram for the ferrite electrode. The two voltammograms did not display any anodic or cathodic peaks and the currents monotonously increased or decreased depending on whether the potential was increasing or decreasing; particularly, their anodic scan curves are almost the same as the cathodic scan curves. This kind of cyclic voltammogram can explain why the polarization

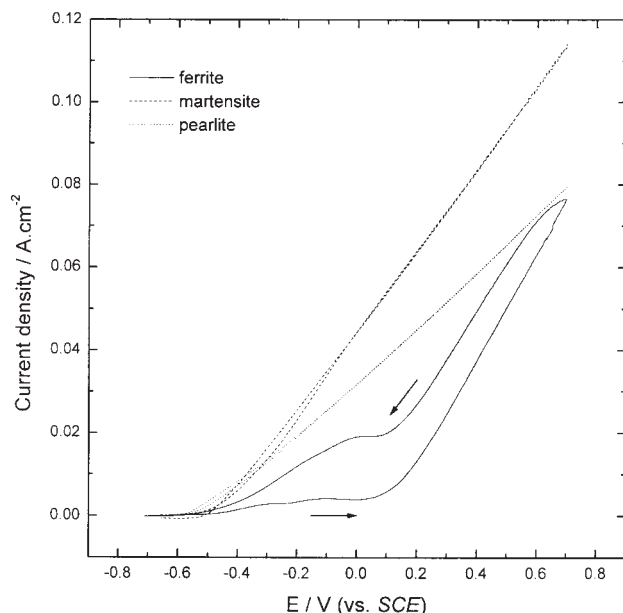


Fig. 1. Cyclic voltammograms of ferrite, martensite and pearlite electrodes scanned at 5 mVs^{-1} in $0.1 \text{ mol dm}^{-3} \text{ Na}_2\text{SO}_4 + 0.1 \text{ mol dm}^{-3} \text{ NaNO}_3 + 0.01 \text{ mol dm}^{-3} \text{ NaCl}$ solutions.

behaviour and surface state of the martensite or pearlite at the same anodic potential are similar regardless of whether the potential was scanned positively or negatively to this potential. It can be inferred from the potential dependence of the current that the surface of the martensite or pearlite remained in the active state; theoretically, pitting should not occur in this case. In fact, no pits were observed on the surface of either of these materials. This means that nitrate ions prevent pitting of martensite and pearlite in neutral sulphate solutions, although they do not render the martensite or pearlite surface passive.

Further comparison of the three cyclic voltammograms shows that, at relatively high potentials, the anodic dissolution rate of martensite is the highest, followed by pearlite and ferrite.

$0.095 \text{ mol dm}^{-3} \text{ Na}_2\text{SO}_4 + 0.005 \text{ mol dm}^{-3} \text{ H}_2\text{SO}_4 + 0.1 \text{ mol dm}^{-3} \text{ NaNO}_3 + 0.01 \text{ mol dm}^{-3} \text{ NaCl}$ solutions ($\text{pH } 2.2$). The anodic dissolution current and the shape of the cyclic voltammogram for ferrite were strongly dependent on the pH of the solution, as shown by the solid line in Fig. 2. However, compared with ferrite, the shape of the cyclic voltammograms for both martensite and pearlite exhibited little change only their anodic dissolution current densities were enhanced with decreasing pH. The pH decrease made the anodic current density of ferrite the highest, martensite next and pearlite the lowest, among these three materials.

Here focus is mainly on the cyclic voltammetric result of the ferrite. During the anodic scan, the anodic current increased rapidly with potential until it reached a maximum at 0.78 V , and further increase of the potential led to a steep drop in the current, as well as passivation of the ferrite surface. From 0.94 V to more positive potentials, the current density remained at a magnitude of approximately $10^{-4} \text{ A cm}^{-2}$. This indicates that the passivation of the ferrite surface was not destroyed by the chloride ions in the presence of nitrate ions. In other words, NO_3^- ions are able to inhibit pitting of the iron caused by chloride ions in acidic sulphate solutions. When the potential was scanned back to the corrosion potential, the cathodic scan

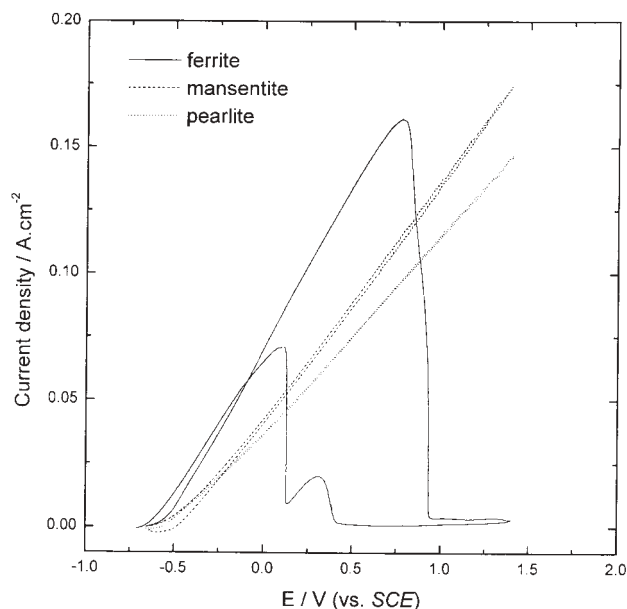


Fig. 2. Cyclic voltammograms of ferrite, martensite and pearlite electrodes scanned at 5 mV s^{-1} in $0.095 \text{ mol dm}^{-3} \text{ Na}_2\text{SO}_4 + 0.005 \text{ mol dm}^{-3} \text{ H}_2\text{SO}_4 + 0.1 \text{ mol dm}^{-3} \text{ NaNO}_3 + 0.01 \text{ mol dm}^{-3} \text{ NaCl}$ solutions.

curve showed a current maximum in the potential range between 0.42 V and 0.13 V. The passive film on ferrite in acidic sulphate solutions is known to be a bilayer film composed of an inner Fe_3O_4 layer and an outer Fe_2O_3 layer.¹³ With decreasing applied potential, the outer layer is reduced and dissolved first, followed by the inner layer. The current maximum is therefore associated with the dissolution of the inner Fe_3O_4 layer. At 0.13 V, the current density increased sharply since the passive film dissolved completely.

It is of interest that no pits were observed on the surface of the ferrite, martensite or pearlite in acidic solutions. This indicates that none of the materials underwent pitting corrosion.

$0.2 \text{ mol dm}^{-3} \text{ H}_2\text{SO}_4 + 0.1 \text{ mol dm}^{-3} \text{ NaNO}_3 + 0.01 \text{ mol dm}^{-3} \text{ NaCl}$ solutions ($\text{pH } 1.2$). The anodic current densities of ferrite, martensite and pearlite were promoted more significantly in strong acidic solutions and the shape of their cyclic voltammograms changed greatly as can be seen in Fig. 3, as opposed to those displayed by Figs. 1 and 2. The voltammogram for the ferrite shows that, when the potential was scanned positively, the anodic current increased with the potential until strong periodic current oscillations occurred. This was followed by a sharp drop until, finally, a constant magnitude of approximately $10^{-4} \text{ A cm}^{-2}$ was maintained over a wide potential region due to the formation of a passive film. Oxygen evolution on the electrode commenced at potentials over 1.57 V, causing an increase in the current. When the potential was swept from the positive vertex to the corrosion potential, the curve of the reverse scan coincided almost exactly with the forward scan curve in the potential range when oxygen evolution occurred. The oxygen evolution reaction stopped when the potential had been reduced to 1.57 V. The passivity held until the potential had been reduced to 0.360 V. The reverse curve did not display a current peak like the maximum shown by solid line in Fig. 2 since the dissolution process of the

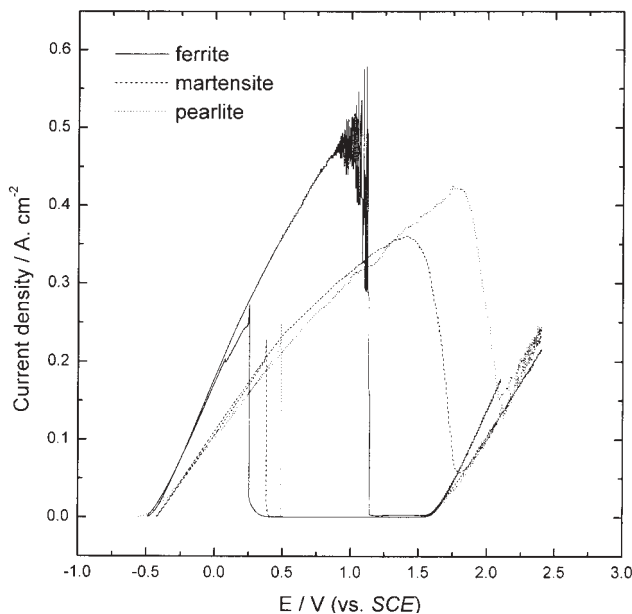


Fig. 3. Cyclic voltammograms of ferrite, martensite and pearlite electrodes scanned at 5 mV s^{-1} in $0.2 \text{ mol dm}^{-3} \text{ H}_2\text{SO}_4 + 0.1 \text{ mol dm}^{-3} \text{ NaNO}_3 + 0.01 \text{ mol dm}^{-3} \text{ NaCl}$ solutions.

passive film was faster in the lower pH solutions.

The cyclic voltammograms for martensite and pearlite were similar to that of ferrite except no current oscillations were observed, involving the current increase with potential, the oxygen evolution, passivation as well as the breakdown of the passive films.

By comparing Figs. 1 through 3, it can be concluded that nitrate is able to inhibit the pitting on ferrite only in acidic solutions, but that its inhibition of pitting on martensite and pearlite is pH independent.

Polarization curves

Steady-state polarization measurements for ferrite, martensite and pearlite were carried out in the three above-mentioned sulphate solutions of different pH in order to investigate the effect of pH on the corrosion behaviour of the three materials. At potentials near the corrosion potentials, the three materials undergo general corrosion rather than pitting.

In the neutral sulphate solution, the polarization curve of ferrite (solid line in Fig. 4) had a linear anodic region between -0.51 V and -0.36 V whose Tafel slope was about 0.086 V/decade , as well as a very wide cathodic plateau from -0.80 V to -0.60 V resulting from the reduction of oxygen dissolved in the solution. The cathodic polarization curves for both martensite and pearlite (see dashed line and dotted line in Fig. 4) were quite different from that of ferrite, not showing the cathodic plateau. The anodic polarization curve for pearlite displayed an approximate linear region of 0.076 V/decade in the potential range from -0.67 V to -0.52 V . No obvious anodic Tafel region was observed from the anodic polarization curve of martensite.

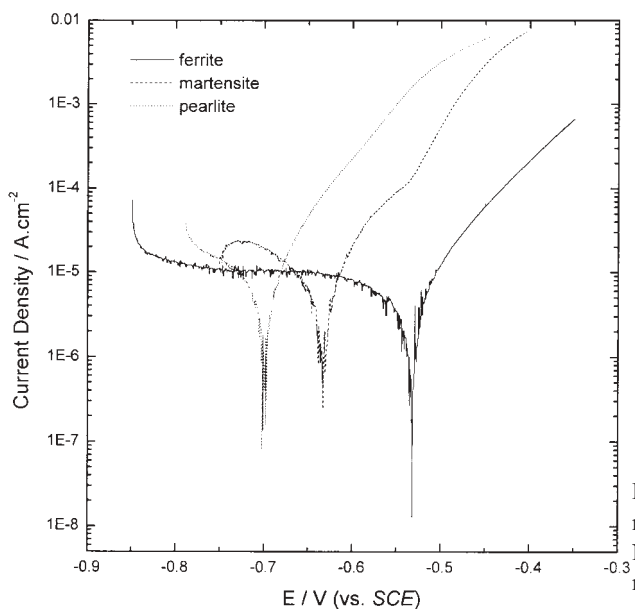


Fig. 4. Polarization curves of ferrite, martensite and pearlite in $0.1 \text{ mol dm}^{-3} \text{ Na}_2\text{SO}_4 + 0.1 \text{ mol dm}^{-3} \text{ NaNO}_3 + 0.01 \text{ mol dm}^{-3} \text{ NaCl}$ solutions.

In the $0.095 \text{ mol dm}^{-3} \text{ Na}_2\text{SO}_4 + 0.005 \text{ mol dm}^{-3} \text{ H}_2\text{SO}_4 + 0.1 \text{ mol dm}^{-3} \text{ NaNO}_3 + 0.01 \text{ mol dm}^{-3} \text{ NaCl}$ solutions, the cathodic and anodic current densities for the three test materials were promoted simultaneously to varying degrees, thereby accelerating their corrosion rate (see Fig. 5). In the acidic solution, the whole cathodic reaction of the three materials is comprised of the oxygen reduction and hydrogen evolution reactions. The anodic dissolution rate of ferrite was enhanced the most by the pH decrease, followed by

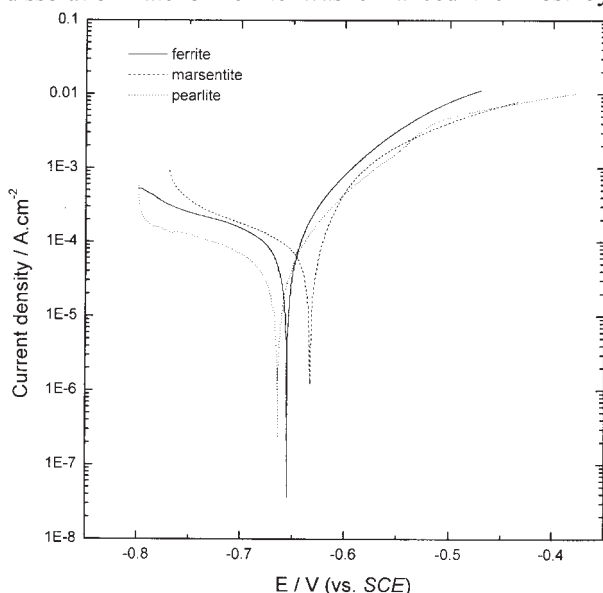


Fig. 5. Polarization curves of ferrite, martensite and pearlite in $0.095 \text{ mol dm}^{-3} \text{ Na}_2\text{SO}_4 + 0.005 \text{ mol dm}^{-3} \text{ H}_2\text{SO}_4 + 0.1 \text{ mol dm}^{-3} \text{ NaNO}_3 + 0.01 \text{ mol dm}^{-3} \text{ NaCl}$ solutions.

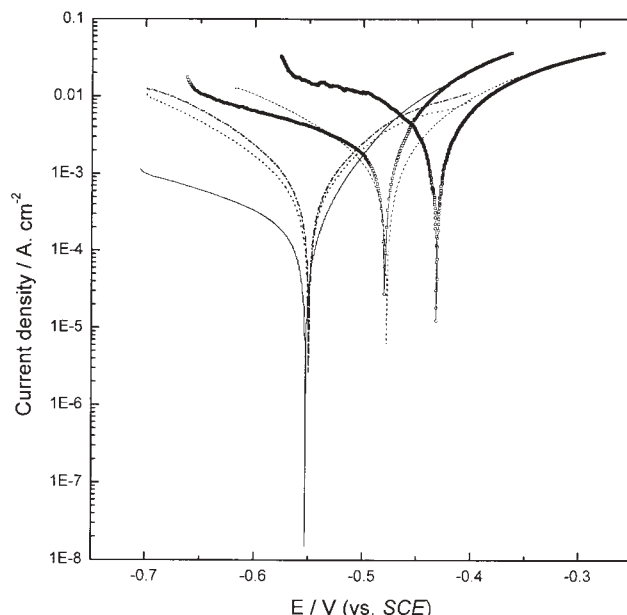


Fig. 6. Polarization curves of ferrite, martensite and pearlite in $0.2 \text{ mol dm}^{-3} \text{ H}_2\text{SO}_4$ solutions in the presence of NaCl and NaNO_3 . (—) Ferrite in $0.2 \text{ mol dm}^{-3} \text{ H}_2\text{SO}_4 + 0.01 \text{ mol dm}^{-3} \text{ NaCl}$; (□) ferrite in $0.2 \text{ mol dm}^{-3} \text{ H}_2\text{SO}_4 + 0.1 \text{ mol dm}^{-3} \text{ NaNO}_3 + 0.01 \text{ mol dm}^{-3} \text{ NaCl}$; (---) martensite in $0.2 \text{ mol dm}^{-3} \text{ H}_2\text{SO}_4 + 0.01 \text{ mol dm}^{-3} \text{ NaCl}$; (○) martensite in $0.2 \text{ mol dm}^{-3} \text{ H}_2\text{SO}_4 + 0.1 \text{ mol dm}^{-3} \text{ NaNO}_3 + 0.01 \text{ mol dm}^{-3} \text{ NaCl}$; (.....) pearlite in $0.2 \text{ mol dm}^{-3} \text{ H}_2\text{SO}_4 + 0.01 \text{ mol dm}^{-3} \text{ NaCl}$; (- - - -) pearlite in $0.2 \text{ mol dm}^{-3} \text{ H}_2\text{SO}_4 + 0.1 \text{ mol dm}^{-3} \text{ NaNO}_3 + 0.01 \text{ mol dm}^{-3} \text{ NaCl}$.

martensite, and then pearlite, the dissolution rate of which was increased slightly. The cathodic curve of ferrite can be divided into two parts: one begins at the corrosion potential and ends at -0.76 V , corresponding to cathodic oxygen reduction; and the other starts at -0.76 V up to more negative potentials, giving a slope of 0.130 V/decade , which is ascribed to cathodic hydrogen evolution. The anodic curve of ferrite exhibits a 0.078 V/decade Tafel slope in the potential range between -0.63 V and -0.54 V , deviating from the result of Bockris, Dražić and Despić (about 0.040 V/decade)¹⁴ and of Heusler (0.030 V/decade) in pure sulphuric acid.¹⁵ The difference between the Tafel slopes reveals a change of the ferrite dissolution mechanism. The cathodic polarization curves of martensite and pearlite were similar to that of ferrite, while the anodic curves of both materials presented no apparent linear region.

In the lower pH acidic solution ($0.2 \text{ mol dm}^{-3} \text{ H}_2\text{SO}_4 + 0.1 \text{ mol dm}^{-3} \text{ NaNO}_3 + 0.01 \text{ mol dm}^{-3} \text{ NaCl}$ solution), the anodic and cathodic reaction rates of ferrite, martensite and pearlite were further accelerated. The polarization curves of the three materials in $0.2 \text{ mol dm}^{-3} \text{ H}_2\text{SO}_4 + 0.1 \text{ mol dm}^{-3} \text{ NaNO}_3 + 0.01 \text{ mol dm}^{-3} \text{ NaCl}$ solutions are shown in Fig. 6. In order to investigate the influence of NO_3^- ions on the general corrosion, the polarization curves of ferrite, martensite and pearlite in $0.2 \text{ mol dm}^{-3} \text{ H}_2\text{SO}_4 + 0.01 \text{ mol dm}^{-3} \text{ NaCl}$ solution were drawn as reference curves in this plot. Obviously, the presence of NaNO_3 has a different influence on the polarization behaviour of the three materials. NO_3^- greatly accelerates both the anodic dissolution current and the cathodic current of ferrite. However, the effect of NO_3^- on the corrosion behaviour of martensite seems to be less than on ferrite. Particularly, NO_3^- has little influence on the polarization behaviour of pearlite.

Impedance spectra

The Nyquist impedance spectra for ferrite, martensite and pearlite in $0.1 \text{ mol dm}^{-3} \text{ Na}_2\text{SO}_4 + 0.1 \text{ mol dm}^{-3} \text{ NaNO}_3 + 0.01 \text{ mol dm}^{-3} \text{ NaCl}$ solutions are shown in Fig. 7. The impedance display of pearlite was a near perfect semicircle. It was calculated from the semicircle that the charge-transfer resistance of the pearlite corrosion reaction is $1466.9 \Omega \text{ cm}^2$ and the double-layer capacitance of the iron surface is $1.01 \times 10^{-3} \text{ F cm}^{-2}$ by fitting the impedance spectrum. The impedance diagrams of both ferrite and martensite presented somewhat distorted semicircles that converted into tails in the low frequency range. It was estimated from the two irregular semicircles that the charge-transfer resistance of ferrite is $1777.3 \Omega \text{ cm}^2$ and that of martensite is $882.4 \Omega \text{ cm}^2$. The charge-transfer resistance may be used to evaluate the ability of one material to resist corrosion. The smaller the charge-transfer resistance, the more easily is the material corroded. It follows from the values of the charge-transfer resistance that the susceptibility of the three materials to general corrosion follows the orders martensite > pearlite > ferrite.

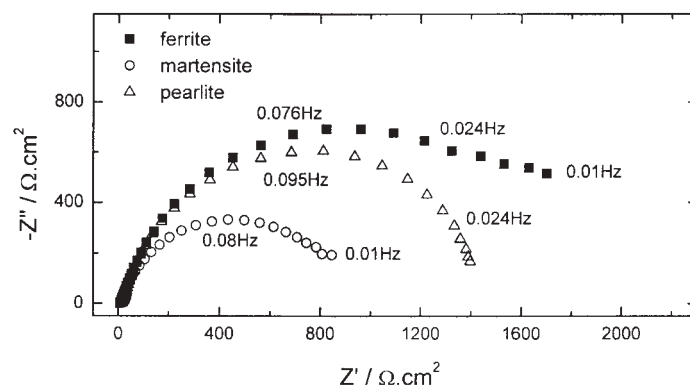


Fig. 7. Nyquist impedance diagrams for ferrite, martensite and pearlite electrodes at their corrosion potentials in $0.1 \text{ mol dm}^{-3} \text{ Na}_2\text{SO}_4 + 0.1 \text{ mol dm}^{-3} \text{ NaNO}_3 + 0.01 \text{ mol dm}^{-3} \text{ NaCl}$ solutions.

Nitrate ions greatly stimulated the general corrosion of ferrite, martensite and pearlite in acidic sulphate solutions, as shown by the impedance plots of the three materials (Figs. 8 and 9). The impedance plot of ferrite shown in Fig. 8 gave three loops, two capacitive loops and one inductive loop; moreover, the shape of the impedance plot is almost independent of the immersion time. The diameter of the high frequency semicircle decreased by $71.7 \Omega \text{ cm}^2$. The impedance spectra for martensite and pearlite are dependent on the immersion time. However, the variation trend of the impedance spectra for the two materials with the immersion times is exactly opposite. For martensite, the impedance plot obtained after 5-minute immersion was a near perfect semicircle; the impedance spectrum developed into one plot with a high frequency capacitive loop and a low frequency inductive loop in 0.5 h, reducing in size and greatly changing in shape. Subsequently, the shape and size of the impedance spectrum did not change with increasing the immersion time (see "□" and "Δ" symbols in Fig. 8). For pearlite, the impedance plot displayed a high frequency capacitive loop and a low frequency inductive one after short immersion (5 min) and a larger capacitive loop after long immersion

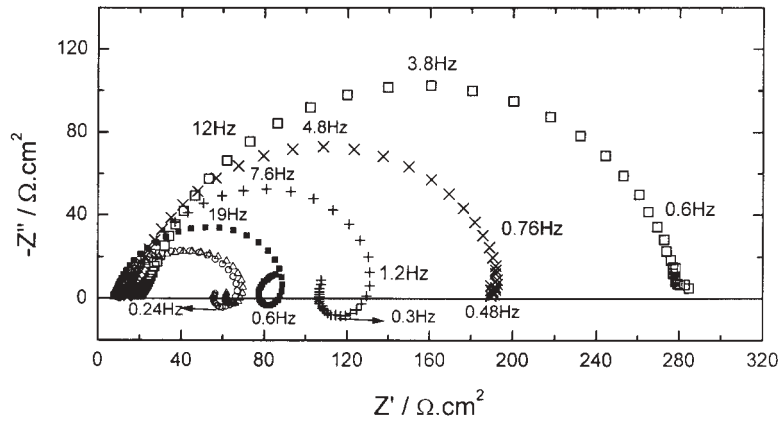


Fig. 8. Nyquist impedance spectra for ferrite, martensite and pearlite electrodes exposed to $0.095 \text{ mol dm}^{-3} \text{ Na}_2\text{SO}_4 + 0.005 \text{ mol dm}^{-3} \text{ H}_2\text{SO}_4 + 0.1 \text{ mol dm}^{-3} \text{ NaNO}_3 + 0.01 \text{ mol dm}^{-3} \text{ NaCl}$ solutions for different times at the open circuit potentials. (■) Ferrite, 5-minute immersion; (□) martensite, 5-minute immersion; (Δ) martensite, 0.5-hour immersion; (○) martensite, 1-hour immersion; (+) pearlite, 5-minute immersion; (×) pearlite, 1-hour immersion.

(1 h). By comparing the impedance spectra of the three materials, it can be concluded that in acidic sulphate solutions containing both nitrate and chloride ions, the order that the three materials undergo general corrosion is martensite, ferrite and pearlite. This conclusion is supported by the results shown in Fig. 9.

Although nitrate ions accelerate the general corrosion of the three materials in acidic solutions, the impedance behaviour of the three materials is somewhat different. Many factors, such as the composition of a material, changes of the surface state, surface roughness or defects, can influence the impedance display of one material. It was observed that the surface of martensite and pearlite gradually became black with increasing immersion time. This could be attributed to the fact that iron and other active metals dissolve in the acidic solutions (see Table I), leaving the carbon on the surface. This phenomenon was particu-

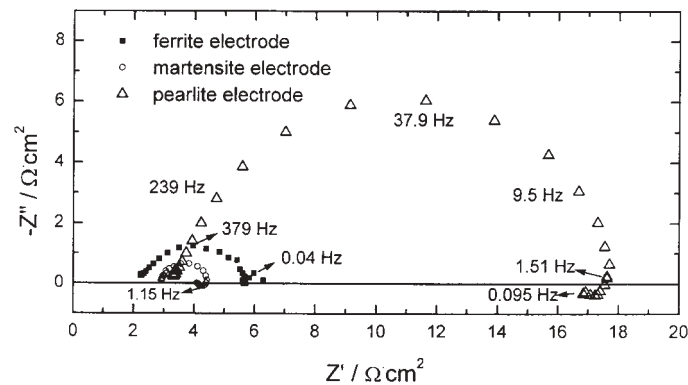


Fig. 9. Nyquist impedance plots for ferrite, martensite and pearlite electrodes in $0.2 \text{ mol dm}^{-3} \text{ H}_2\text{SO}_4 + 0.1 \text{ mol dm}^{-3} \text{ NaNO}_3 + 0.01 \text{ mol dm}^{-3} \text{ NaCl}$ solutions at their corrosion potentials.

larly evident with the martensite electrode. It was observed that more carbon powder was deposited on the martensite surface than on the pearlite surface after identical immersion times in the acidic solution. According to thermodynamic theories, pearlite is an equilibrium phase, whereas martensite is a non-equilibrium phase in which the supersaturated carbon is dissolved in the ferrite phase. The supersaturated carbon has a tendency to separate from the martensite. Consequently, much more carbon appeared on the martensite surface during the immersion in acidic solutions compared with the pearlite one, although the carbon content of the martensite was lower than that of the pearlite, as shown in Table I.

CONCLUSIONS

1. The inhibition of pitting on ferrite by nitrate ions strongly depends on the pH of the solution. Nitrate ions were unable to prevent ferrite from pitting attack in neutral Cl^- -containing Na_2SO_4 solution, whereas in acidic Na_2SO_4 solutions or in H_2SO_4 solutions, nitrate ions completely inhibited pitting on passivated ferrite.

2. Martensite and pearlite were not passivated in neutral $0.1 \text{ mol dm}^{-3} \text{Na}_2\text{SO}_4 + 0.1 \text{ mol dm}^{-3} \text{NaNO}_3 + 0.01 \text{ mol dm}^{-3} \text{NaCl}$ solution or in $0.095 \text{ mol dm}^{-3} \text{Na}_2\text{SO}_4 + 0.005 \text{ mol dm}^{-3} \text{H}_2\text{SO}_4 + 0.1 \text{ mol dm}^{-3} \text{NaNO}_3 + 0.01 \text{ mol dm}^{-3} \text{NaCl}$ acidic solution. Particularly, their anodic scan curves were almost the same as the cathodic scan ones. In the lower pH solution ($0.2 \text{ mol dm}^{-3} \text{H}_2\text{SO}_4 + 0.1 \text{ mol dm}^{-3} \text{NaNO}_3 + 0.01 \text{ mol dm}^{-3} \text{NaCl}$), the two materials can be passivated. Pitting did not occur on the surface of these two materials in sulphate solutions, irrespective of the pH values.

3. In different pH sulphate solutions, the polarization measurements and impedance spectra obtained at the corrosion potentials show that the pH strongly affected the rate of general corrosion of ferrite, martensite and pearlite. In neutral solutions, the corrosion rate of martensite is the highest, followed by that of pearlite and ferrite. However, in acidic sulphate solutions, the corrosion rate of the three materials is in the order martensite, ferrite and pearlite.

Acknowledgements: This project is supported by the Special Funds for the Major State Basic Research Projects G 19990650 and the Chinese National Science Fund (20173033).

ИЗВОД

УПОРЕЂЕЊЕ УТИЦАЈА НИТРАТНОГ ЈОНА НА ЕЛЕКТРОХЕМИЈСКО ПОНАШАЊЕ ГВОЖЂА И УГЉЕНИЧНИХ ЧЕЛИКА У СУЛФАТНИМ РАСТВОРИМА

HOUYI MA¹, SHENHAO CHEN^{1,2}, CHAO YANG³ и JINGLI LUO³

¹Department of Chemistry, Shandong University, Jinan, 250100, P. R. China, ²State Key Laboratory for Corrosion and Protection of Metal, Shenyang, 110015, P. R. China and ³Department of Chemical and Materials Engineering, University of Alberta, Edmonton, Alberta, Canada, T6G 2G6

Утицај нитратног јона на електрохемијско понашање гвожђа (ферита) и два угљенична челика (мартензит и перлит) испитиван је у сулфатним растворима различитог рН цикличном волтаметријом, одређивањем поларизационих кривих и импедансном спектроскопијом. Ин-

хибициони ефекат нитратног јона на појаву питинга код ферита је зависан од рН. Нитратни јони не спречавају појаву питинга на фериту у неутралним растворима, али врло ефикасно штите пасивиран ферит од питинга у киселим сулфатним растворима. На површинама мартензита и перлита нема појаве питинга у сулфатним растворима, без обзира на рН раствора. На потенцијалима отвореног кола (корозиони потенцијал) сва три материјала подлежу општој корозији. Импедансни спектри сва три материјала одређени за неутралне сулфатне растворе који садрже нитрате и хлориде показују капацитивне петље, док су спектри у киселим сулфатним растворима значајно смањени по величини и показују нискофреквентне импедансне петље (индуктивне или капацитивне петље) поред добро познатих капацитивних петљи у области виших фреквенција. Дато је објашњење промене импедансе са променом рН.

(Примљено 21. јануара 2002)

REFERENCES

1. Z. Szklarska-Smialowska, *Pitting Corrosion of Metals*, NACE, Houston, 1986, p. 4
2. N. Cui, L. J. Qiao, J. L. Luo, S. Chiovelli, *Br. Corros. J.* **35** (2000) 210
3. H. Y. Ma, N. Cui, J. L. Luo, S. Chiovelli, *Appl. Surf. Sci.* (submitted)
4. R. C. Newman, M. A. A. Ajjawi, *Corros. Sci.* **12** (1986) 1057
5. H. H. Uhlig, J. R. Gilman, *Z. Phys. Chem.* **226** (1964) 127
6. W. Schwenk, *Corrosion* **20** (1964) 129t
7. G. Herbsleb, *Werkst. Korros.* **16** (1965) 929
8. K. J. Vetter, H. H. Strehblow, Ber. Bunsenges, *Physik. Chem.* **74** (1970) 449
9. H. H. Strehblow, B. Titze, *Corros. Sci.* **17** (1977) 461
10. H. P. Leckie, H. H. Uhlig, *J. Electrochem. Soc.* **113** (1966) 1261
11. Z. Szklarska-Smialowska, *Pitting Corrosion of Metals*, NACE, Houston, 1986, p. 283
12. Z. Szklarska-Smialowska, *Pitting Corrosion of Metals*, NACE, Houston, 1986, p. 44
13. X. L. Cheng, C. Wang, X. Chen, S. H. Chen, *J. Serb. Chem. Soc.* **61** (1996) 917
14. J. O'M. Bockris, D. Dražić, A. R. Despić, *Electrochim. Acta* **4** (1961) 326
15. K. E. Heusler, *Z. Elektrochem.* **62** (1958) 582.